Supplementary Materials for

A gut-brain neural circuit for nutrient sensory transduction

Melanie Maya Kaelberer, Kelly L. Buchanan, Marguerita E. Klein, Bradley B. Barth, Marcia M. Montoya, Xiling Shen, Diego V. Bohórquez*

Corresponding author. Email: diego.bohorquez@duke.edu

Published 21 September 2018, *Science* **361**, eaat5236 (2018)
DOI: 10.1126/science.aat5236

This PDF file includes:

Other Supporting Online Material for this manuscript includes the following:
(available at www.sciencemag.org/content/361/6408/eaat5236/suppl/DC1)

Movies S1 and S2
Data S1 as zipped archive

Materials and Methods

Animals. Mouse care and experiments were carried out in accordance with protocols approved by the Institutional Animal Care and Use Committee at Duke University Medical Center under the protocol A009-16-01. Mice were housed in the Duke University animal facilities, where they were kept on a 12-hour light dark cycle. They received food and water *ad libitum*. The following strains were used: C57Bl6 (4-12 weeks), Cck-GFP (4-12 weeks), Pgp9.5-GFP (4-12 weeks). Double transgenic mice were all bred in house: CckCRE_tdTomato (6-12 weeks), CckCRE_ChR2-tdTomato (6-12 weeks), PyyCRE_rabG-Tva (P8), Phox2bCRE_GCaMP6s (6-12 weeks), CckCRE_rabG-Tva (P8), PyyCRE_tdTomato (6-12 weeks), CckCRE_Halo-YFP (6-12 weeks), and Vglut1CRE_ChR2-YFP (6-12 weeks). Mouse strains and their sources:

Mouse strain	**Source**	**Stock Number**
C57Bl6	Jackson Lab	000664
Cck-GFP	Courtesy of Rodger Liddle	Wang *et al.,* 2010 (*30*)
Pgp9.5-GFP	Jackson Lab	024355
CckCRE	Jackson Lab	012706
PyyCRE	Courtesy Andrew Leiter	Schonhoff *et al.*, 2005 (*31*)
Phox2bCRE	Jackson Lab	016223
Vglut1CRE	Jackson Lab	023527
LSL_tdTomato	Jackson Lab	007914
LSL_ChR2-tdTomato	Jackson Lab	012567
LSL_ChR2-YFP	Jackson Lab	007612
LSL_rabG-Tva	Jackson Lab	024708
LSL_GCaMP6s	Jackson Lab	024106
LSL_Halo-YFP	Jackson Lab	014539

*LSL=loxP-STOP-loxP cassette

Rabies production. G-deleted rabies virus production was performed in house as described in Wickersham et. al (*28*). For rescue from cDNA, B19G cells were plated on 10 cm dishes in DMEM with 10% FBS, Glutamax, and NEAA on the day before transfection. At 85%

confluence, the cells were transfected using Lipofectamine2000 (Invitrogen) with genome vector 38 µg cSPBN-4GFP (Addgene 52487) or 38 µg pRVdG-4mCherry (Addgene 52488), 18 µg pCAG B19N (Addgene 59924), 9 µg pCAG B19P (Addgene 59925), 7.5 µg pCAG B19G (Addgene 59921), 9 µg pCAG B19L (Addgene 59922), and 11 µg pCAG T7 pol (Addgene 59926). The following day the media was changed to DMEM with 2% FBS, GM, NEAA and Sodium pyruvate. Viral supernatants were collected every three days while the cells remained healthy. Supernatants were filtered with a 0.45 µm filter and concentrated by ultracentrifugation at 26K-rpm through a 20% sucrose cushion. If necessary, viral stocks were further amplified on B19G cells. EnvA pseudotyped virus was prepared by infecting BHK-EnvARGCD2 cells with G-deleted B19G rabies virus. The next day, the cells were rinsed twice with PBS, exposed to 0.25% trypsin for 5 minutes and re-plated on new 10 cm dishes. One day later the cells were again rinsed twice with PBS. Supernatant was collected every three days, 0.45 µm filtered, and concentrated by ultracentrifugation.

Organoid culture. Organoids were cultured using a protocol adapted from Sato *et al.*, 2009 (*29*). The small intestines of CckCRE_tdTomato or wild-type mice were dissected and flushed twice with cold PBS. The intestine was cut open lengthwise and cut again into ~1 cm pieces. Tissue pieces were incubated with 1.5 mM EDTA at 4˚C for 15 minutes then at 37˚C for 15 minutes. New cold PBS was added, and crypts were mechanically detached. Crypts were spun down and re-suspended in Matrigel (Corning #356231). Crypts in Matrigel were plated 50 µl per well in a 24-well plate. After 15 minutes' incubation at 37˚C, 500 µl of media were added to each well. Organoid media contains 1x Glutamax, 10 10mM HEPES, 200U/ml Penicillin-Streptomycin, 1x N2 supplement, 1x B27 supplement, 0.25ng/ml EGF, 50ng/ml Noggin, and 100ng/ml r-Spondin in Advanced DMEM/f12.

Rabies tracing. For colon monosynaptic tracing, P1 mice were given a 10 µl enema of EnvA-ΔG-rabies-GFP (5.9×10^9 ffu/ml). The experimental mice used were PyyCRE_rabG-Tva (n=9), with negative CRE genotype littermates as controls (n=4). One control mouse was not included in the data set due to extensive colon damage caused by the enema. For small intestine monosynaptic tracing, P1 mice were given a 50 µl gavage of ΔG-rabies-GFP (9.8×10^8 ffu/ml). The experimental mice used were CckCRE_rabG-Tva (n=3), with negative CRE genotype littermates as controls (n=2). Mice were sacrificed 7 days after exposure at P8. Tissue harvested included the colon (or stomach and small intestine), lumbar/sacral DRGs, nodose ganglia, and brain. Tissue was post-fixed in 4% PFA for three hours and then treated with serial sucrose solutions of 10%, 20%, and 30%. Ganglia were whole-mount imaged with a multiphoton microscopy system (Bruker Ultima IV with a Chameleon Vision II tunable laser). All other tissue was frozen in OCT blocks and sectioned for immunohistochemistry.

Enteroendocrine cell and nodose neuron co-culture. The small intestines of CckGFP and CckCRE_Chr2-tdTomato mice were dissected and flushed twice with cold PBS. The intestine was cut open lengthwise and cut again into ~1 cm pieces. Tissue pieces were incubated with 3 mM EDTA at 4˚C for 15 minutes then at 37˚C for 15 minutes. New cold PBS was added, and villi and crypts were mechanically detached. Villi and crypts were spun down and further digested in Collagenase and Dispase. Cells were spun down and re-suspended in L-15 media

with 5% FBS and DNase to prevent cell clumping. Cells were passed through a 70 µm then 40 µm cell strainer to isolate single cells. Then cells were sorted using Fluorescence Activated Cell sorting (BD FACSAria) selecting for GFP, or tdTomato, fluorescent cells. Cells were sorted into organoid culture media (listed above) plus 10ng/ml NGF. Sorted cells were plated on Matrigel coated 12mm coverslips at a concentration of ~5-10k enteroendocrine cells per coverslip. Nodose neurons were dissected and incubated with Liberase (Roche) digestion enzyme. Enzyme was washed off and replaced with media. Single cells were dissociated by mechanical force and filtered through a 70µm cell strainer. Neurons in media were plated evenly on up to 8 coverslips with enteroendocrine cells. Patch-clamp electrophysiology was performed 2-5 days after plating.

Immunohistochemistry. Tissue sections were cut at a thickness of 10-18µm, then post-fixed in 10% NBF for 10 minutes and washed in TBS + 0.05% Tween20 (TBST). Sections were blocked with 10% Donkey Serum for 1 hour prior to being incubated overnight at 4˚C with primary antibody [Rb-Anti-PYY [DVB3] (1:1000); Rb-Anti-CCK (1:1000; courtesy of Rodger Liddle or Phoenix Pharmaceuticals H-069-04); Gt-Anti-PSD95 (1:500; Santa Cruz Biotechnology: sc-6926); Rb-Anti-Syn1 (1:500; Cell Signaling Technology: 5297S); Ck-Anti-GFP (1:500; Abcam: ab13970]. After TBST washes, sections were incubated with secondary antibody (Jackson ImmunoReseach) for one hour at room temperature [Dk-Anti-Rb-488 (1:250); Dk-Anti-Rb-Cy3 (1:250); Dk-Anti-Gt-Cy5 (1:250); Dk-Anti-Ck-488 (1:250)]. Slides were washed with TBST, then incubated with DAPI and mounted for imaging. Imaging was done on a Zeiss 880 Airyscan inverted confocal microscope. Data are presented as the mean percentage ± S.E.M.

Real-time quantitative PCR. The small intestinal epithelium of Cck-GFP mice was dissociated and cells were sorted as described above. An equal number of GFP+ and GFP- cells were collected directly into lysis buffer. Nodose was dissected and flash frozen in liquid nitrogen. For all tissue, RNA was extracted based on the manufacturer's protocol using the RNeasy Micro Plus Kit (Qiagen #74034). Then cDNA was produced per manufacturer's protocol using the High Capacity cDNA Reverse Transcription Kit (Applied Biosystems #4368814). The following TaqMan probes were used for transcript identification:

Gene	**TaqMan ID**	**Gene**	**TaqMan ID**
18S	Mm03928990_g1	*Lrrtm2*	Mm00731288_s1
Cask	Mm00438021_m1	*Nrxn1*	Mm00660298_m1
Cck	Mm00446170_m1	*Nrxn2*	Mm01236851_m1
Efnb2	Mm00438670_m1	*Nrxn3*	Mm04279482_m1
Gria1	Mm00433753_m1	*Pyy*	Mm00520716_g1
Gria2	Mm00442822_m1	*Reg4*	Mm00471115_m1
Gria3	Mm00497506_m1	*Sct*	Mm01275684_g1
Grik3	Mm01179716_m1	*Slc17a6*	Mm00499876_m1
Grik5	Mm00433774_m1	*Slc17a7*	Mm00812886_m1

Grin1	Mm00433790_m1	*Slc5a1*	Mm00451203_m1
Grm7	Mm01189424_m1	*Slc5a2*	Mm00453831_m1
Grm8	Mm00433840_m1	*Syn1*	Mm00449772_m1
Lrrc4	Mm01166846_s1		

Real-time qPCR was run on a StepOnePlus System (Thermo Fischer), using TaqMan Fast Universal PCR Master Mix (Applied Biosystems #4352042) according to the manufacturer's protocol. Transcription rate was determined as $2^{-\Delta Ct}$, or compared as fold-change over EEC negative epithelial cells using $2^{-\Delta\Delta Ct}$. All values are reported as mean ± S.E.M.

Electrophysiology. Enteroendocrine cells and nodose neurons were co-cultured as described above. Co-culture coverslips were placed in the recording chamber filled with extracellular solution. Recordings were carried out at room temperature using a MultiClamp 700B amplifier (Axon Instruments), digitized using a Digidata 1550A (Axon Instruments) interface, and pClamp software (Axon Instruments) for data acquisition. Data was filtered at 1 kHz and sampled at 10 kHz. CCK-producing enteroendocrine cells were identified by GFP expression and neurons by their morphology and lack of fluorescence. Recordings were made using borosilicate glass pipettes pulled to ~3.5 MΩ resistance. Extracellular solution contained (in mM): 140 NaCl, 5 KCl, 2 CaCl2, 2 MgCl2, 10 HEPES, pH 7.4 (300- 305 mOsmol). For voltage-clamp recordings, intracellular solution contained (in mM): 140 CsF, 10 NaCl, 0.1 CaCl2, 2 MgCl2, 1.1 EGTA, 10 HEPES, 10 sucrose (pH, 7.25, 290 - 295 mOsmol). For current-clamp recordings, intracellular solution contained (in mM): 140 KCl, 0.5 EGTA, 5 HEPES, 3 Mg-ATP, 10 sucrose (pH, 7.25, 290 - 295 mOsmol). Neurons were held at -70 mV for 5 min after patching in voltage-clamp mode (to stabilize cells), and then switched to the current-clamp mode. At the resting membrane potential, cell properties such as input resistance, and spike threshold were determined using 200 ms steps from -40 pA to 100 pA in 20 pA increment. After that, baseline neuron activity was recorded in current-clamp or voltage-clamp for 5 min before exposure to glucose (10-20mM) for 30-60 sec, followed by a wash with no glucose-containing extracellular solution. After glucose exposure, neurons were tested with a current or voltage pulse to confirm the health of the cell. For glutamate receptor blocker experiments, the SmartSquirt Microperfusion system (Automate Scientific, Inc.) was used. Once the neuron was patched, the SmartSquirt nozzle was brought to within 100µm of the cell, while extracellular solution was perfusing. Kynurenic acid (3mM) was perfused, then washed for 5 minutes after and the neuron was tested again. EPSC responses were recorded for 1 second after light stimulation. Data are presented as the mean ± S.E.M. and significance was determined using a two-tailed Student's t test.

iGLuSnFR stable cell line. The 5.2Kb iGluSnFR (pCMV(MinDis).iGluSnFR was a gift from Loren Looger; Addgene plasmid # 41732) was moved to the zeocin resistant backbone of Addgene #51694 (DRH296: FCK-Optopatch2 was a gift from Adam Cohen) as a NdeI + XhoI fragment. The resulting plasmid (pMEK8) was transfected into HEK 293/17 cells (ATCC CRL-11268) using 1ul Lipofectamine 2000/ug DNA. Cells were maintained in DMEM (Gibco 11965) supplemented with 10% FBS (Corning 35-010-CV), Glutamax, non-essential amino acids (both Gibco) and 3ul/ml zeocin (100ng/ml, Invitrogen) (*27*).

iGluSnFR-HEK cell and enteroendocrine cell co-culture, and imaging. CckCRE_tdTomato enteroendocrine cells were isolated as described above. Isolated cells were mixed with iGluSnFR-HEK cells at a ratio of 10:1, then plated on 1% Matrigel coated coverslips. Control iGluSnFR-HEK cells were plated alone. Cells were incubated for 12-18 hours before imaging. Coverslips were imaged using a multiphoton microscopy system (Bruker Ultima IV with a Chameleon Vision II tunable laser). Imaging frames were captured at 1.876 fps, using 920nm light. Imaging series were analyzed using Fiji (it's just ImageJ), and cell traces were plotted with Excel.

Vagus nerve recording. Wild-type control (n = 5-9), CckCRE_ChR2-tdTomato (n=6), CckCRE_Halorhodopsin-YFP (n = 5), and Vglut1CRE_ChR2-YFP (n = 6) mice were used for vagal recordings. Mice were anesthetized with 3mg/g-mouse urethane 1 hour before surgery then with 0.5-1% isoflurane. A section of neck skin was removed between the jaw and clavicle. The thyroid was reflected bilaterally, and the carotid bundle was exposed using coarse dissection. The carotid nerve was separated from the vagus nerve using a curved blunt probe. Two platinum iridium wires (0.001" diameter, PTFE coated, 10% Ir 90% Pt; Medwire by Sigmund Cohn Corp) were looped around the vagus nerve for recording. Mineral oil was used to insulate the vagus nerve from surrounding tissue. The small intestine was exposed by removing a section of skin and peritoneum. A 20-gauge gavage needle was surgically inserted through the stomach wall and into the duodenum. The gavage needle was sutured in place beyond the pyloric sphincter. Saline and stimulant tubes were connected to the gavage needle. For optogenetic experiments, a fiber optic cable (FT020, ThorLabs) was threaded through the gavage needle into the lumen of the duodenum. A perfusion exit incision was made 10 cm distal to the pyloric sphincter. During each recording, PBS was constantly perfused through the duodenum using a peristaltic pump (Cole-Parmer) at the lowest setting for a flow rate of ~400uL PBS per minute. Stimulation conditions were applied after recording 2 minutes of baseline activity. During nutrient stimulation conditions, PBS perfusion was continuous, and 200 µL of stimulant (**Ensure®**, 1M sucrose, 500mM fructose, 500mM D-glucose, or 2.9µM CCK octapeptide-sulfated (BaChem)) was perfused through the second tube for 1 minute using a syringe pump (Fusion 200, Chemyx) for a final concentration of ~300mM sucrose in PBS (600-700 mOsm), ~150mM D-glucose in PBS (~500mOsm), ~150mM fructose in PBS (~500mOsm), and ~ 870nM CCK in PBS (10µg/kg dose). Final stimulant concentrations were determined using the ratio of dilution and confirmed by osmolarity testing (Model 3320 Osmometer, Advanced Instruments Inc.). During 473 nm laser stimulation conditions, PBS perfusion was continuous, and the laser was pulsed for 1 minute at 40 Hz, 4 volts peak voltage, 20% duty cycle (473nm, 80 mW laser, RGBlase).

Antagonist studies. To observe the effects of phloridzin dehydrate (Sigma), devazepide (Sigma), kynurenic acid (Sigma), and DL-2-Amino-3-phosphonopropionic acid (AP-3, Sigma) on vagal nerve firing rate, response to sucrose, 473nm laser, or CCK was recorded before and after antagonist delivery. All antagonists were delivered intraluminally over 1 minute in 200µL solution via the gavage needle inserted into the duodenum, noting the duodenal perfusion exit incision released all inhibitors into the peritoneal cavity. For experiments using the SGLT1 inhibitor, phloridzin was dissolved into 1M sucrose solution at a concentration of 0.4% w/v (8.47 mM) and was delivered like other stimulants for a final phloridzin concentration of ~3mM. For

experiments using devazepide the CCK-A receptor antagonist, devazepide was dissolved in DMSO and diluted in PBS for a final dose of 2mg/kg in 200µL solution. To validate the dose based on previously published reports, devazepide dose was titrated to fully attenuate vagal response to CCK (870nm, 10µg/kg) (Fig. S18); a dose of 1mg/kg did not fully attenuate the response (data not shown). Following a 5-minute incubation period, stimulant recordings continued for up to 1 hour with no return of CCK response. For experiments using the glutamate receptor antagonists, stock solutions of kynurenic acid and AP-3 were dissolved in 1M NaOH, and experimental concentrations were diluted in PBS, pH=7.4. Doses were determined based on previously published results: 1mg/kg AP-3 and 150µg/kg kynurenic acid(*35, 36*). A dose response curve was acquired for kynurenic acid 1.5ug/kg- 1.5mg/kg validating the chosen dose (Fig. S20). For glutamate cocktail experiments, 200µL of each inhibitor were delivered simultaneously for a total volume of 400µL. Following dose, stimulant recording experiments were initiated immediately. Effect of inhibitor persisted 10-15 minutes (data not shown). Therefore, each post-inhibitor data point for the glutamate inhibitors was from the recording directly following glutamate inhibitor application. Inhibitors were re-dosed as necessary throughout recording.

Data Acquisition: Extracellular voltage was recorded from a pair of platinum iridium wires as described. A differential amplifier and bandpass filter (1000X gain, 300 Hz – 5kHz bandpass filter; A-M Systems LLC) was used and the signal was processed using a data acquisition board and software (20 kHz sampling rate; Signal Express, National Instruments Corp). The raw data was analyzed using a spike sorting algorithm (MATLAB by MathWorks). Spikes were detected using simple threshold detection based on RMS noise. The firing rate was calculated using a Gaussian kernel smoothing algorithm (200-ms time scale) (*37*).

Statistical Methods: Stimulation response was quantified as the maximum firing rate after stimulation (stimulant conditions) or during recording (baseline). For stimulant conditions, additional parameters were quantified. Time to peak was calculated as time from start of stimulus to maximum firing rate. Area under the curve was calculated as area under the curve for the entire 6-minute recording. Each trial served as its own control by normalizing the maximum firing rate to the average baseline firing rate (defined as the first two minutes of recording, prior to stimulation onset). Mice were excluded from analysis if no sucrose response was present throughout recording. Maximum firing rate, time to peak, and area under curve are analyzed across genotype, stimulation condition, and their interaction term by ANOVA, followed by Tukey HSD post hoc testing (JMP by SAS Institute).

Eating behavior assay. Experimental (n=3), CckCRE_ChR2, or control (n=5) mice at 8-12 weeks old were used. An abdominal window was surgically implanted in order to gain access to the small intestine (distal duodenum/ proximal jejunum) (*38*). Mice were given 3 days to recover from the surgery and re-establish their normal eating behavior. Mice were then fasted overnight and the next day were anesthetized with 1-2% isoflurane and a laser was used to stimulate the small intestine through the window, either 437nm for experimental, or 532nm, or no laser, for the control (80 mW laser, RGBlase). The laser stimulation was pulsed at 40 Hz, 20% duty cycle for 30 minutes. Then mice were observed for 2 hours after recovery from anesthesia, while the number of food pellets eaten was recorded. Significance was determined using a two-tailed Student's t test.

Fast Blue tracing. Wild-type mice (6 weeks old) were given a 50µl enema of Fast Blue (2mg/ml) (Polysciences, Inc). For vagotomy experiments, the mice were anesthetized and the right cervical vagus was cut. Mice were sacrificed 5 days' post enema and tissue was collected and fixed for imaging.

Calcium imaging. For neurons, Phox2bCRE_GCaMP6s (n=3) nodose neurons were dissociated and plated as previously described (*39*). Briefly, nodose ganglia were dissected and digested in Liberase (Roche, 5401054001). Neurons were washed and filtered through a 70µm cell strainer, then plated on 12mm coverslips and placed in an incubator overnight. Cells were imaged 1-2 days later. Coverslips were placed in the recording chamber of a Zeiss Examiner Z1 and imaged with a Hamamatsu camera (Orca-flash4.0; C11440) using the Zeiss ZEN software package. For enteroendocrine cells, CckCRE_tdTomato organoids with transduced with *ΔG*-rabies-GCaMP6s. Organoids were imaged using multiphoton microscopy 3-4 days after transduction. Imaging buffer (in mM: 140 NaCl, 5 KCl, 2 $CaCl_2$, 2 $MgCl_2$, 10 HEPES) was continuously perfused over the coverslips. Glucose (20mM) was perfused for 30 seconds, then washed and KCl (40mM) was applied for 30 seconds as an activity control. Images were analyzed with Fiji (it's just ImageJ), and cell traces were plotted with Matlab.

Single Cell Western Blot Analysis. CckGFP cells were dissociated and cell sorted as outlined above. The Milo single-cell Western Blot (Protein Simple) was used according to the manufacturers protocol and previously established technique (*40*). Cells were loaded onto a micro-well gel by distributing the ~40k cell suspension onto the gel and through gravity cells settled into wells over 25 minutes. The chip was run through the Milo (10 sec lysis, 60 sec separation, followed by UV light for 3 min to stop the gel run). Gel was probed with two antibodies: 1-Rabbit anti-synapsin-1 (Cell Signaling #5297) at 1:10 dilution and Donkey anti-rabbit IgG Alexa 647 at 1:20 dilution; 2-Goat anti-GFP (Abcam #ab6673) at 100µg/ml and Donkey anti-goat IgG Alexa 555 at 1:20 dilution. Chips were imaged with a microarray scanner and analyzed in Scout software (Protein Simple). Each lane was imaged in two channels and the area under the detected peak was used to quantify the target abundance in each cell.

Mass Spectrometry. *Sample Preparation*. Equal amounts of Cck-GFP cells (~100K cells/n) and non-GFP intestinal epithelial cells were sorted and collected in PBS. Nodose neurons, from both left and right ganglia, of the same mouse were also collected. Cells were spun down, PBS removed and snap frozen in liquid nitrogen. Frozen cells and tissue (n=3 per group) were thawed, and 50µl of 0.25% ALS-1 in 50 mM ammonium bicarbonate, pH 8 was added to each sample followed by sonification. After centrifugation at 15,000 *x g* for 10 min., the supernatant was transferred, and protein recovery was quantified by Bradford assay. After normalization of protein concentration with lysis buffer, samples were denatured and reduced by addition of 10mM DTT and heated at 80˚C for 10 min., followed by alkylation with 20mM iodoacetamide in the dark for 30 min. Sequencing grade modified trypsin (Promega; 1:50 w/w trypsin:protein) was added, and proteins were digested at 37˚C overnight. Samples were then acidified with 1% trifluoroacetic acid (TFA), 2% acetonitrile (CAN), followed by heating at 60˚C for 2h, to

inactivate trypsin and degrade ALS-1. Trypsinized yeast alcohol dehydrogenase 1 (MassPrep, Waters) was added at 50 fmol per µg as an internal standard to each sample. Following centrigugation, supernatants were transferred to Maximum Recovery LC vials (Waters). QC pools were prepared by mixing equal volumes of all samples.

Quantitative Mass Spectrometry. Since 1978, enteroendocrine cells have been classified under the assumption that one cell would synthesize one hormone only (*5*). Alphabet letters were assigned to different hormone peptides –*S* for secretin, *A* for Ghrelin, *D* for somatostatin– but recent reports show that a single enteroendocrine cell expresses gene transcripts of multiple neuropeptides (*12, 13*). Using quantitative mass spectrometry, we found that purified CCK cells contain significant amounts of at least 10 other neuropeptides including peptide YY, protachykinin-1, and tryptophan hydroxylase 1 (Cck-GFP>10-fold compared to non-GFP epithelial cells; $p < 0.05$; n=3) (Table S1). The last two proteins are often used as markers of the enterochromaffin cell subtype. Therefore, the same enteroendocrine cell can secrete multiple neuropeptides, including both CCK and PYY, which we used in the present article as markers.

The procedure was performed as follows: Quantitative one-dimensional liquid chromatography, tandem mass spectrometry (1D-LC-MS/MS) was performed on 250 ng of the peptide digests per sample in singlicate, with additional QC and conditioning analyses. Samples were analyzed using a nanoAcquity UPLC system (Waters) coupled to a QExactive Plus high resolution accurate mass tandem mass spectrometer (Thermo) via a nanoelectrospray ionization source. Briefly the sample was first trapped on a Symmetry C18 300 mm x 180 mm trapping column (5 µl/min at 99.9/0.1 v/v H_2O/MeCN) followed by an analytical separation using a 1.7 µm Acuity HSS T3 C18 75 mm x 250 mm column (Waters) with a 90-min. gradient of 5 to 40% CAN with 0.1% formic acid at a flow rate of 300 nl/min and column temperature of 55˚C. Data collection on the QExactive Plus mass spectrometer was performed in data-dependent acquisition (DDA) mode of acquisition with an r=70,000 (@ m/z 200) at a target AGC value of 5e4 ions. A 20 s dynamic exclusion was employed. The total analysis cycle time for each sample injection was approximately 2 h. Following 18 total analyses (including conditioning and QC injections), data was imported into Rosetta Elucidator v3.3 (Rosetta Biosoftware, Inc), and all LC-MS runs were aligned based on the accurate mass and retention time of detected ions ("features") using PeakTeller algorithm in Elucidator. Relative peptide abundance was calculated based on area-under-the-curve (AUC) of aligned features across all runs. The overall dataset had 221,597 quantified features, and 610,511 high collision energy (peptide fragment) spectra that were subjected to database searching. This MS/MS data was searched against a custom Swissprot database with *Mus musculus* taxonomy (downloaded on 01/27/15) with additional proteins, including yeast ADH and enhanced GFP, as well as an equal number of reversed-sequence "decoys" for false discovery rate determination (33,404 total entries). Mascot Distiller and Mascot Server (v2.5 Matrix Sciences) were utilized to produce fragment ion spectra and to perform the database searches. Included in the database searches were fixed modification on Cys (carbamidomethyl) and variable modifications on Met (oxidation) and Asn/Gln (deamidation). After individual peptide scoring using PeptideProphet algorithm in Elucidator, the data was annotated at a 0.8% peptide false discovery rate. For quantitative processing, the data was first curated to contain only high-quality peptides with appropriate chromatographic peak shape and the dataset was intensity scaled to the robust mean across all samples analyzed.

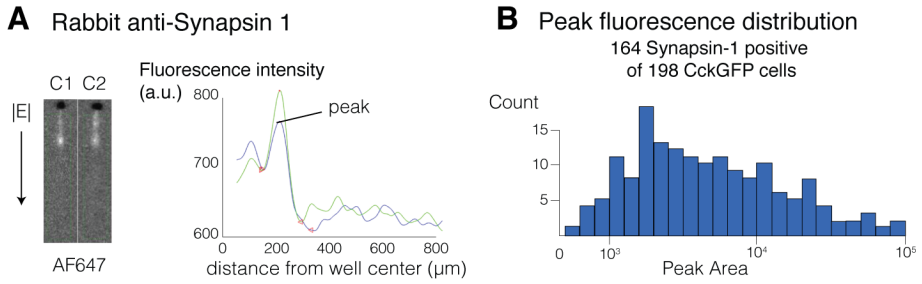

Fig. S1. Single cell Western blot of duodenal enteroendocrine cells. (**A**) Cck-GFP cells were isolated and run on 1mm Western lanes (*left*). Then, probed with Rabbit anti-Synapsin-1 and Chicken anti-GFP antibody. Fluorescence intensity was measured and the area under the peak intensity curve was calculated. (**B**) The peak area corresponds to the amount of protein detected. 164 cells of 198 GFP positive cells (83%) were also positive for Synapsin-1.

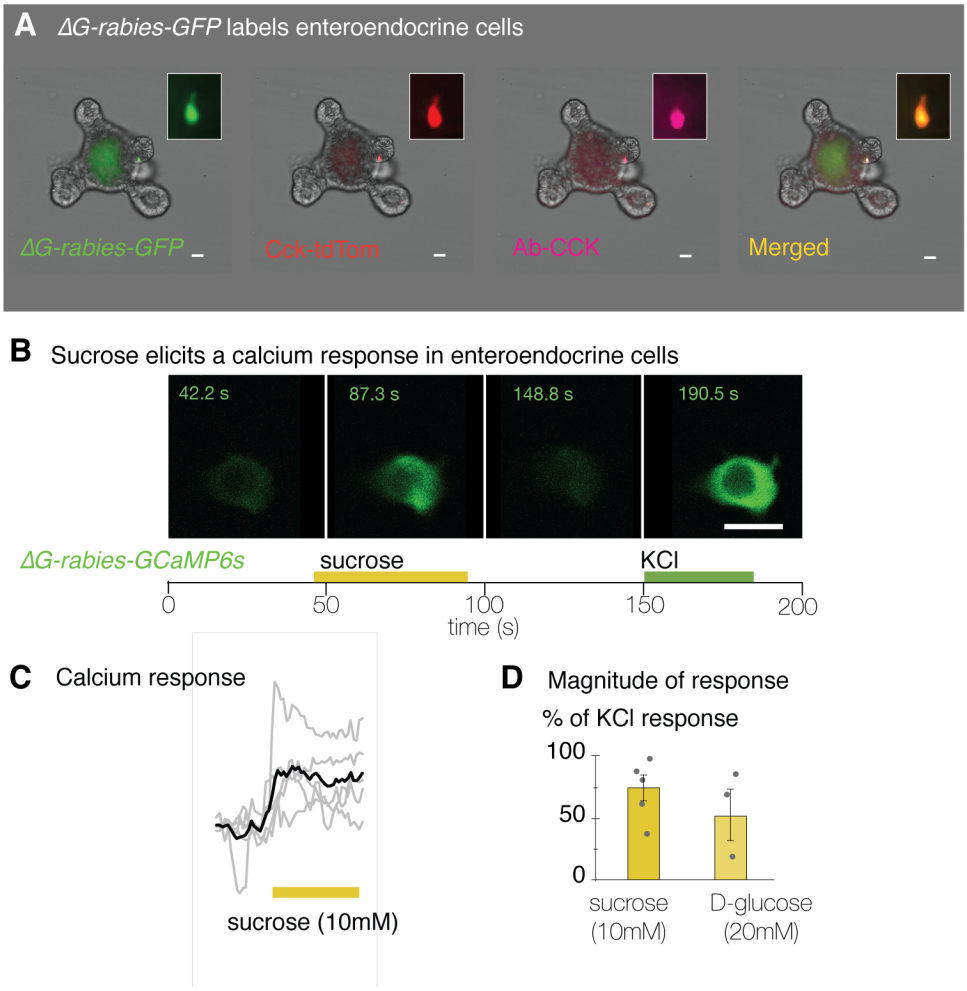

Fig. S2. D-glucose does elicit a calcium response in enteroendocrine cells. (**A**) Δ*G-rabies-GFP* transduces (*first-left*) enteroendocrine cells in CckCRE_tdTomato organoids (*second-left*) as confirmed by antibody staining (*third-left*). (**B**) Organoids from CckCRE_tdTomato mice were transduced with Δ*G-rabies-GCaMP6s*, then imaged using multiphoton microscopy. Cells were given an experimental sugar stimulus (10mM sucrose, or 20mM D-glucose), followed by a wash, then a 40mM KCl control stimuli. (**C**) Fluorescence traces of individual enteroendocrine cells-*grey*, and the average trace across cells-*black*. (**D**) The magnitude of the sugar response was calculated as the percent fluorescence of the KCl response. The sucrose response was calculated to be 72.4±10.6% of KCl (n=5 cells), and the D-glucose response was calculated to be 56.0±20% of the KCl response (n=3 cells). Bars = 10µm.

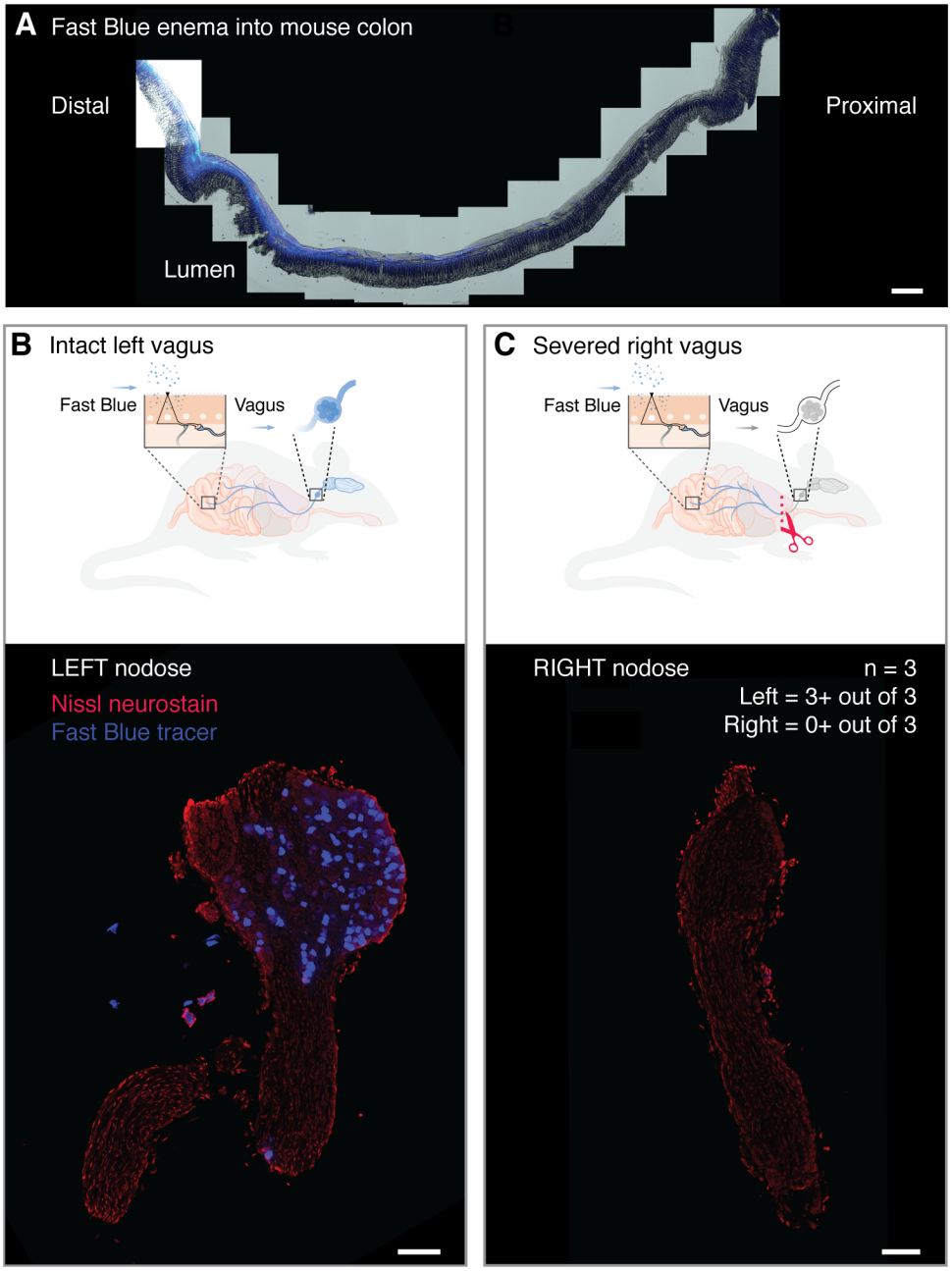

Fig. S3. Fast Blue enema labels vagal neurons innervating the colon. (**A**) Colon cross section of wild-type mice shows that dye is only present in the distal colon. (**B**) The left-control cervical vagus is left intact, and labeled cells are seen in the nodose ganglion (*model-top, image-bottom*). (**C**) The right-experimental cervical vagus is cut at the time of enema. No nodose neurons are labeled on the severed vagus side (n=3 mice) (*top-model, bottom-image*).

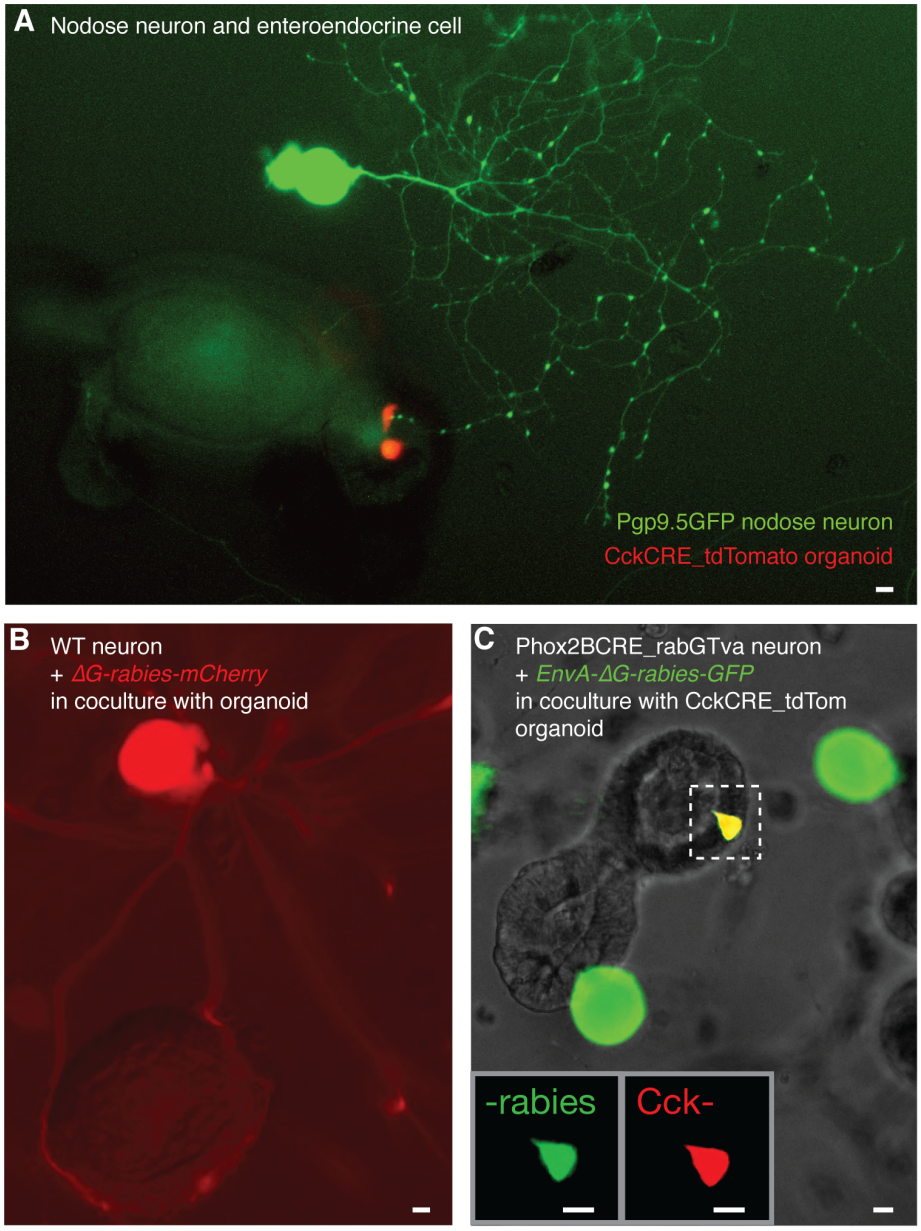

Fig. S4. *In vitro* rabies transfection and retro-tracing in intestinal organoids co-cultured with vagal nodose neurons. (**A**) Co-cultures of PGP9.5-GFP nodose neurons with CckCRE_tdTomato organoids shows that neurons grow out and make contact with CCK cells in organoids. (**B**) Wild-type nodose neurons are transduced by ΔG-rabies-mCherry before culturing with organoids. Wild-type neurons are not able to infect synaptically connected cells. (**C**) Phox2bCRE_rabG-Tva neurons are transduced with EnvA-ΔG-rabies-mCherry before culturing with organoids. Rabies spreads mono-synaptically to transduce connected enteroendocrine cells. Bars = 10µm.

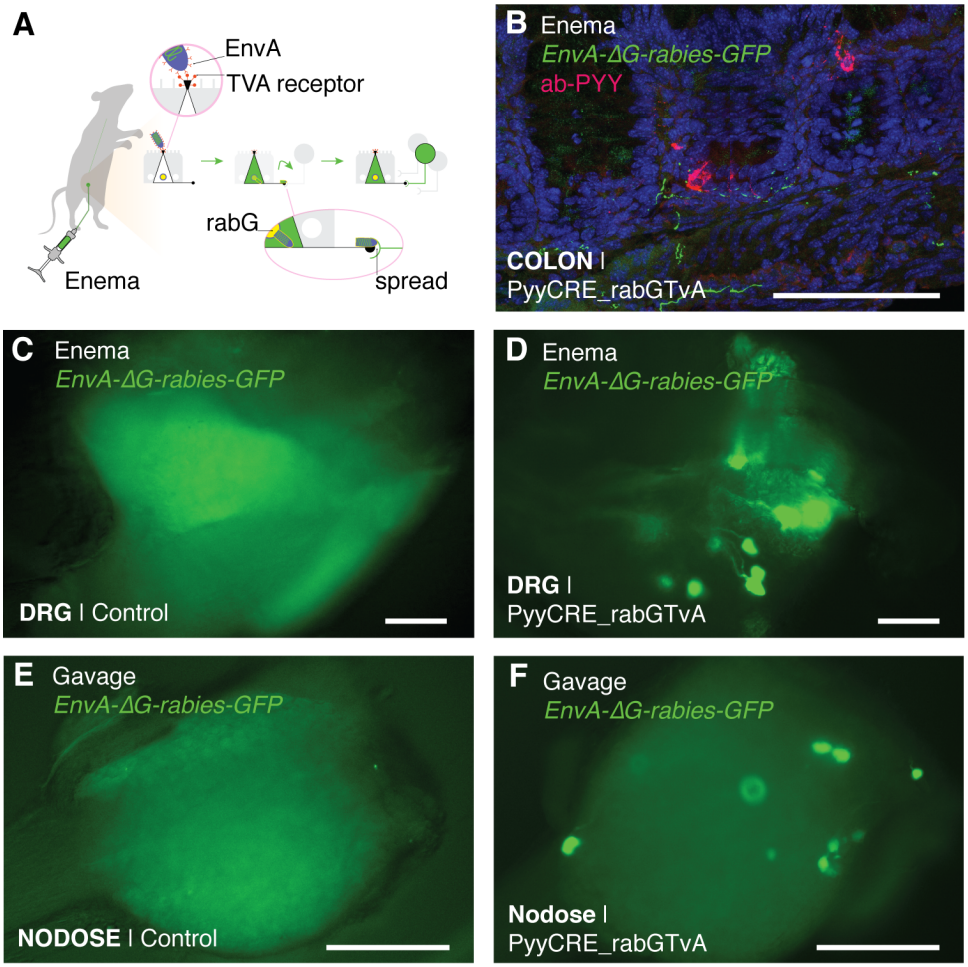

Fig. S5. Monosynaptic rabies tracing from the intestine to sensory ganglia. (**A**) Colon enema of *EnvA-ΔG-rabies-GFP* was performed to trace monosynaptic connections. **(B)** Colon enema of *EnvA-ΔG-rabies-GFP* in PyyCRE_rabG-Tva colon with PYY antibody staining, 5 out of 9 mice were transduced. **(C)** Control mice showed no transduction in dorsal root ganglion control (n=4 control mice). **(D)** Dorsal root ganglion in 4 out of 5 colon transduced mice showed rabies transduction of GFP. (**E**) Gavage of Δ*G-rabies-GFP* in a control mouse nodose showed no transduction. (**F**) Gavage of Δ*G-rabies-GFP* in CckCRE_rabG-Tva mice nodose (n= 2 of 3 mice) showed rabies transduction in the nodose ganglia. Bars = 100μm.

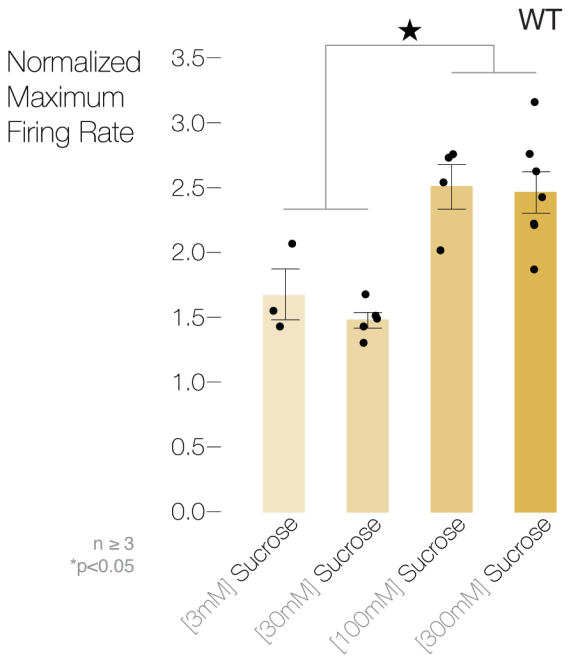

Fig. S6. Vagal firing rate responds to varying sucrose concentrations. Normalized maximum firing rate for 3mM, 30mM, 100mM, an 300mM sucrose in wild-type mice ($n \geq 3$, error bars indicate S.E.M.). Stars indicate significant difference ($p < 0.05$) using ANOVA and Tukey HSD post hoc analysis.

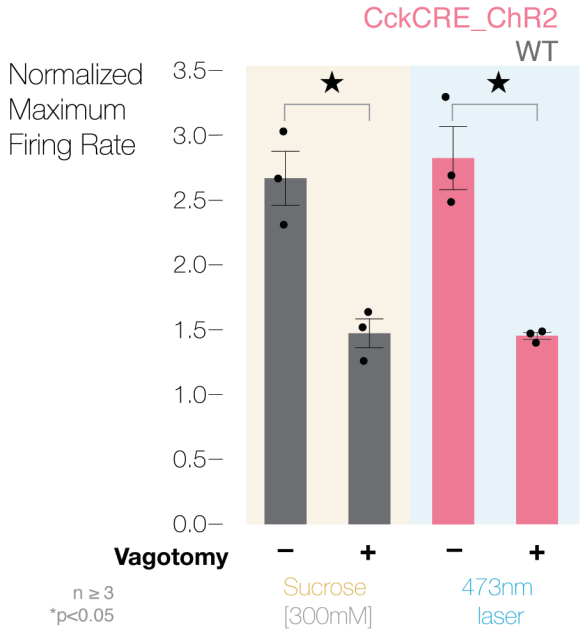

Fig. S7. Sub-diaphragmatic vagotomy attenuates increase in vagal firing rate from sucrose and laser. Normalized maximum firing rate for sucrose-300mM in wild-type mice and intraluminal 473nm laser in CckCRE_ChR2 mice before (-) and after (+) sub-diaphragmatic vagotomy ($n \geq 3$, error bars indicate S.E.M.). Stars indicate significant difference ($p < 0.05$) using ANOVA and Tukey HSD post hoc analysis.

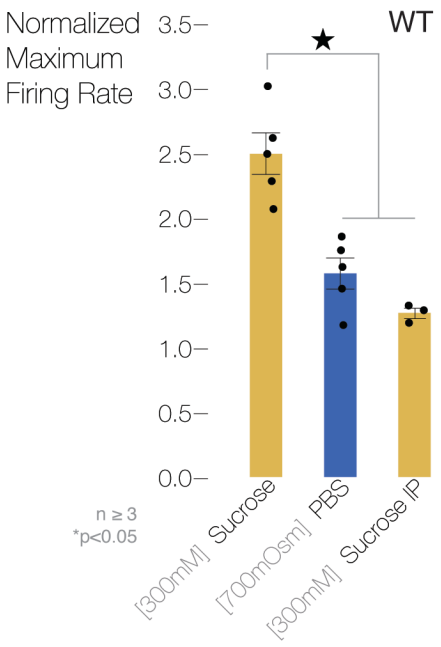

Fig. S8. High osmolarity PBS-700mOsm delivered intraluminally and sucrose-300mM delivered intra-peritoneally (IP) did not increase vagal firing rate. Normalized maximum firing rate for sucrose-300mM intraluminal, PBS-700mOsm intraluminal, and sucrose-300mM IP in wild-type mice ($N \geq 3$, error bars indicate S.E.M.). Star indicates significant difference ($p < 0.05$) using ANOVA and Tukey HSD post hoc analysis.

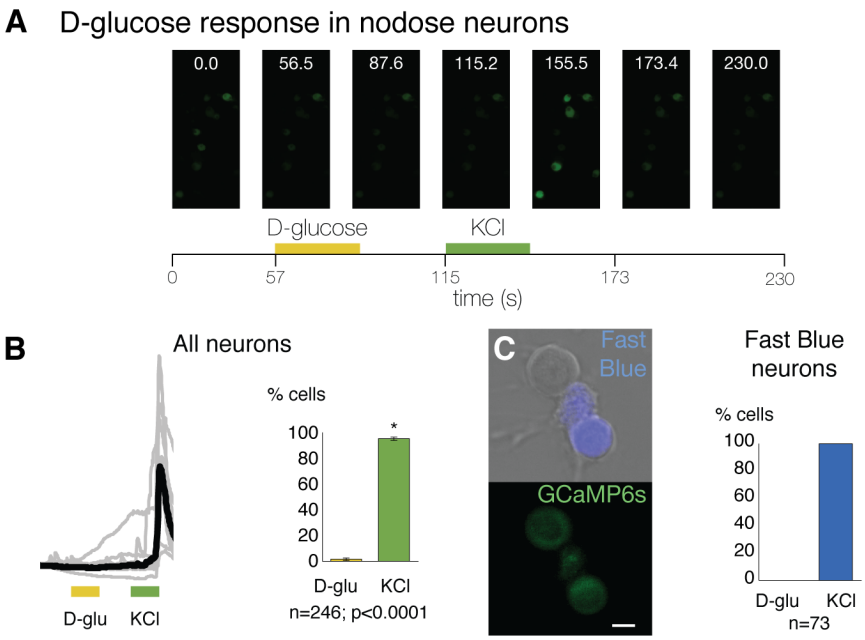

Fig. S9. D-glucose does not elicit a calcium response in nodose neurons. (**A**) Phox2bCRE_GCaMP6s nodose neurons were dissociated and plated for *in vitro* calcium imaging. First an experimental D-glucose (20mM) stimuli was applied followed by a wash then KCl (40mM) as a control stimulus. (**B**) (*left*) Fluorescence traces of cells-*grey*, and the average trace across cells-*black*. Of nodose neurons imaged, 2.7±1.9% responded to glucose and 97.3±1.9% of neurons did not respond to 20mM D-glucose. (mice=3, cells=246, error bars indicate S.E.M., * student's t-test determined p=3.7E-06). (**C**) Nodose neurons that innervate the small intestine were identified by Fast Blue tracing from the proximal duodenum. Calcium imaging of Fast Blue positive neurons showed 100% of neurons did not respond to a 20mM D-glucose stimuli. (mice = 2, cells = 73). Bar = 10µm.

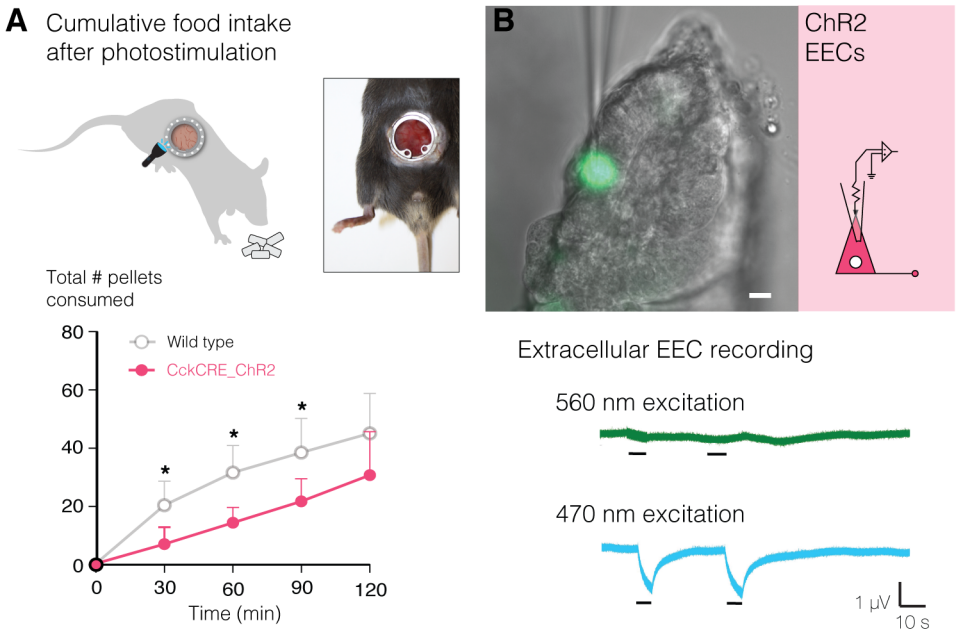

Fig. S10. Enteroendocrine cells in CckCRE_ChR2-tdTomato mice decrease mouse eating behavior when activated and are light sensitive. (**A**) CckCRE_ChR2-tdTomato mice were implanted with an abdominal window (*top*). They were fasted overnight then 473nm laser stimulation was administered through the window for 30 minutes. After stimulation, the number of food pellets cumulatively eaten was measured. CckCRE_ChR2-tdTomato mice ate significantly less than control wild type mice (n=3 experimental, n=5 control, significance was determined using a two-tailed Student's t test). (**B**) In gut sections, CckCRE_ChR2-tdTomato mice were recorded from using extracellular sharp electrode recording. 560 nm light did not elicit activity. Whereas, 470 nm light did elicit a response.

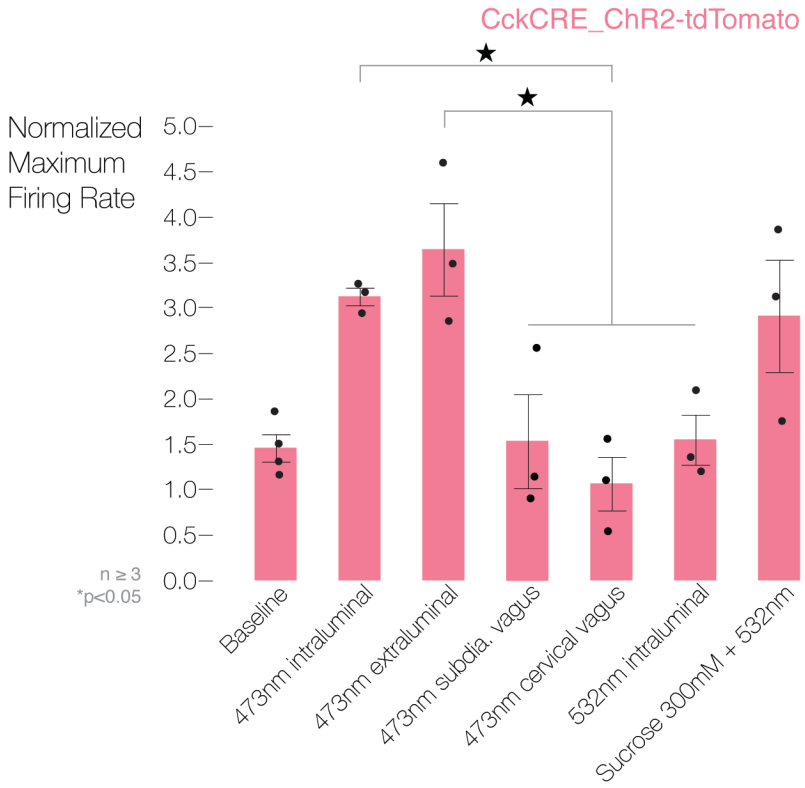

Fig. S11. Vagal firing rate does not respond to laser application at sub-diaphragmatic or cervical vagus in CckCRE_ChR2-tdTomato mice. Normalized maximum firing rate for 473 intraluminal laser, 473nm extraluminal laser, 473nm sub-diaphragmatic vagus, 473nm cervical vagus, 532nm intraluminal, and sucrose-300mM + 532nm laser stimulation in CckCRE_ChR2-tdTomato mice ($n \geq 3$, error bars indicate S.E.M.). Stars indicates significant difference ($p < 0.05$). Statistics by ANOVA and Tukey HSD post hoc analysis.

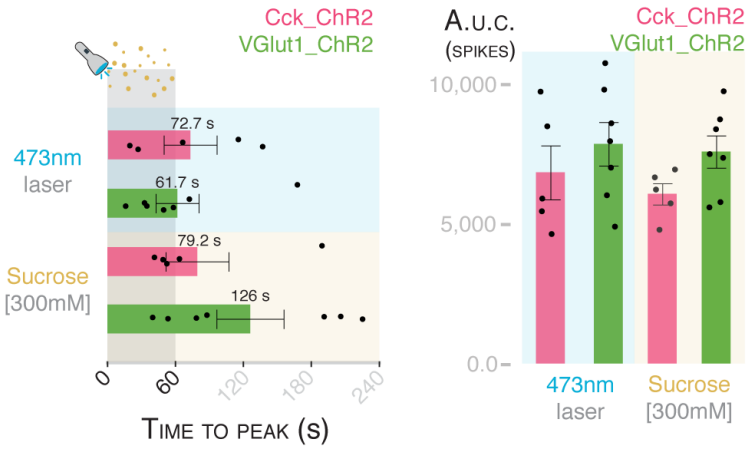

Fig. S12. Vagal firing rate responds rapidly to sucrose and 473nm in CckCRE_ChR2-tdTomato and Vglut1CRE_ChR2-YFP mice. Time to peak and area under the curve (A.U.C.) for sucrose-300mM and 473nm intraluminal laser application in CckCRE_ChR2-tdTomato and Vglut1CRE_ChR2-YFP mice ($n \geq 5$, error bars indicate S.E.M.). No statistical significance. Statistics by ANOVA and Tukey HSD post hoc analysis.

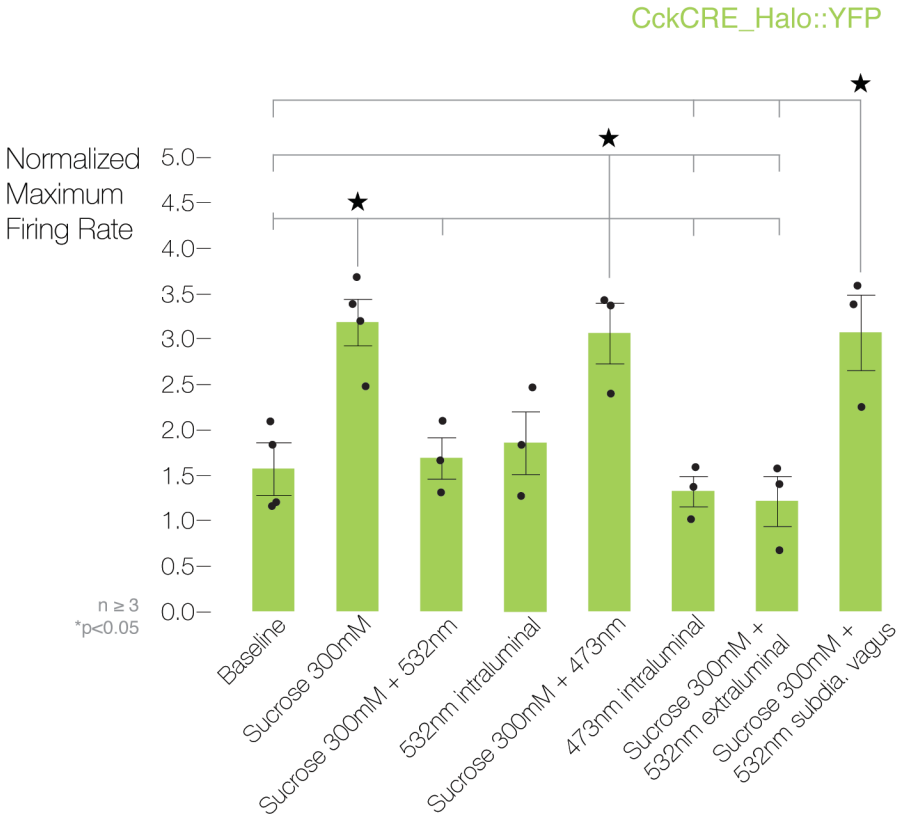

Fig. S13. Vagal firing rate responds sucrose-300mM, sucrose-300mM + 473nm intraluminal laser, and sucrose-300mM + 532nm laser applied to the sub-diaphragmatic vagus in CckCRE_Halo-YFP mice. Normalized maximum firing rate for baseline, sucrose-300mM, sucrose-300mM + 532nm intraluminal laser, 532nm intraluminal laser, sucrose-300mM + 473nm intraluminal laser, 473nm intraluminal laser, sucrose-300mM + 532nm extraluminal laser, and sucrose-300mM + 532nm laser applied to sub-diaphragmatic vagus in CckCRE_Halo-YFP mice ($n \geq 3$, error bars indicate S.E.M.). Stars indicates significant difference ($p < 0.05$). Statistics by ANOVA and Tukey HSD post hoc analysis.

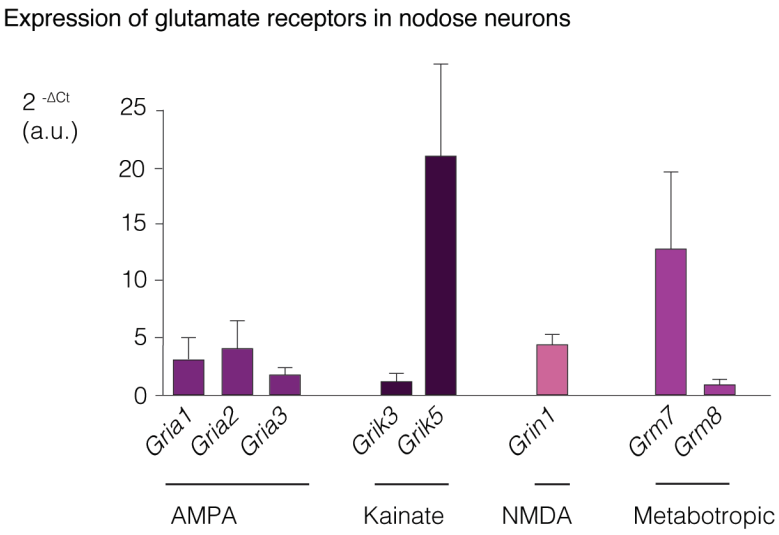

Fig. S14. Real time qPCR expression of glutamate receptors in the nodose ganglia. The nodose ganglia expresses glutamate receptors in each of the four sub-types of receptors: AMPA, kainate, NMDA, and metabotropic. Values are reported as $2^{-\Delta Ct}$ compared to 18S expression (mean ± S.E.M.; n=3).

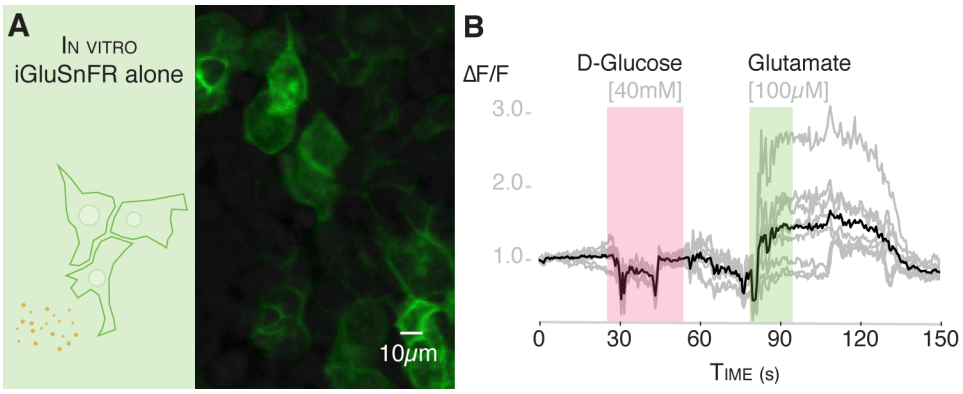

Fig. S15. iGluSnFR-HEK cells respond to glutamate but not D-glucose. **(A)** HEK cells were transfected with the membrane bound iGluSnFR plasmid and cultured (*model-left, image-right*). **(B)** Glutamate-100μm but not D-glucose-40mM causes an increase in fluorescence in iGluSnFR-HEK cells as measured by multiphoton microscopy (n=10 cells).

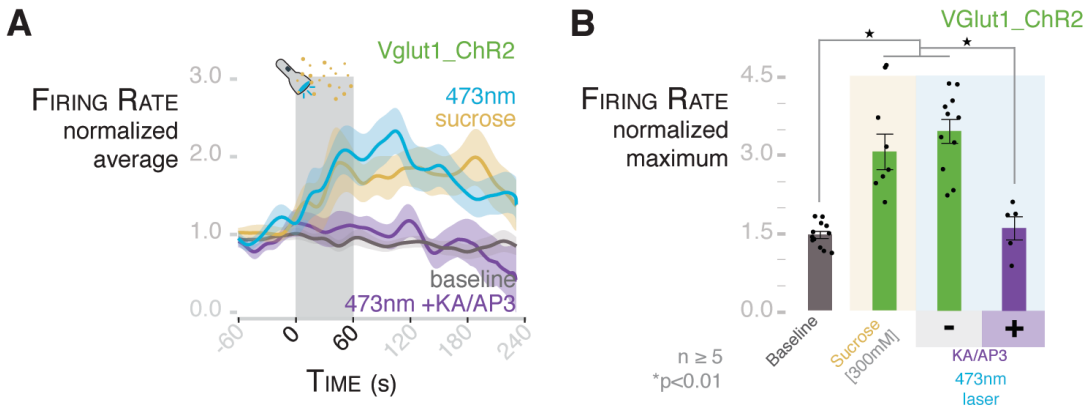

Fig. S16. Activation of VGlut1+ enteroendocrine cells is sufficient to drive a glutamatergic vagal response. **(A)** Normalize traces for baseline, sucrose-300mM, 473nm intraluminal laser, and 473nm intraluminal laser with glutamate inhibitor cocktail (KA/AP3 = 150 µg/kg kynurenic acid + 1 mg/kg AP-3) in Vglut1CRE_ChR2-YFP mice. (**B**) Sucrose and 473nm laser stimulate vagal activity in Vglut1CRE_ChR2. The response to laser is fully attenuated by KA/AP3.

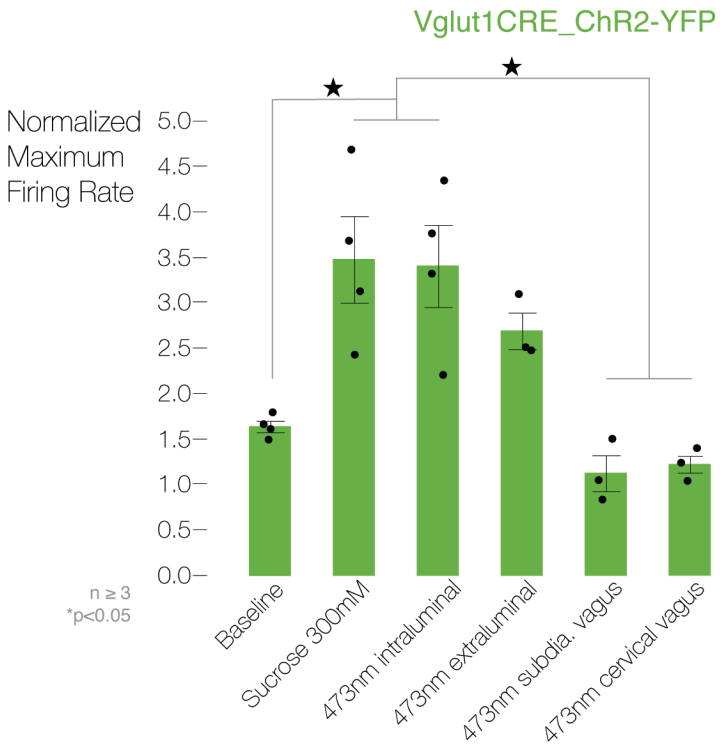

Fig. S17. Vagal firing rate responds to sucrose-300mM, 473nm intraluminal, and 473nm extraluminal laser stimulation in Vglut1CRE_ChR2-YFP mice. Normalized maximum firing rate for 300mM sucrose, and intraluminal, extraluminal, subdiaphragmatic vagus, and cervical vagus laser application in Vglut1CRE_ChR2-YFP mice ($n \geq 3$, error bars indicate S.E.M.). Stars indicates significant difference ($p < 0.05$). Statistics by ANOVA and Tukey HSD post hoc analysis.

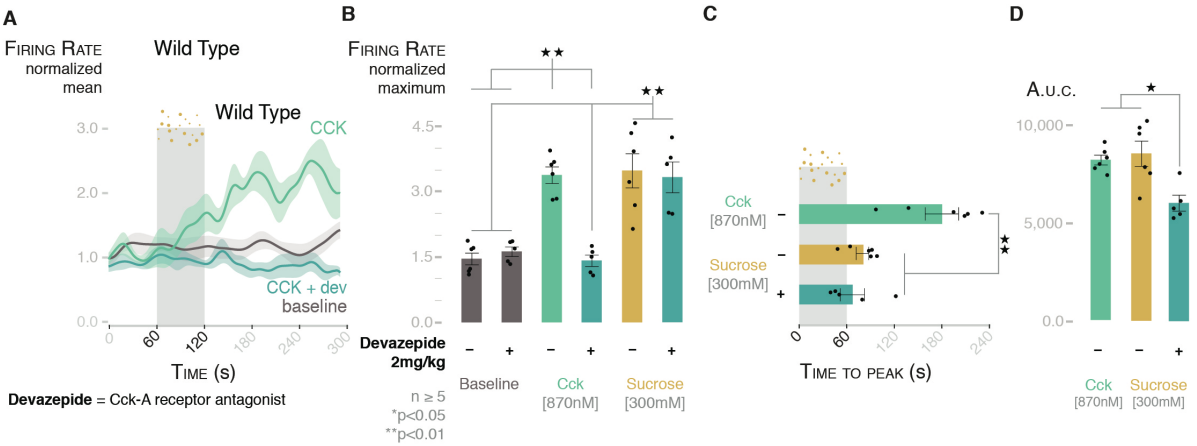

Fig. S18. Devazepide completely attenuates the vagal response to CCK. **(A)** Normalized traces for baseline, CCK-870nM (10µg/kg), and CCK-870nM following devazepide-2mg/kg delivered intraluminally in wild-type mice. **(B)** Normalized maximum firing rate for baseline before and after devazepide, CCK-870nM before and after devazepide, and sucrose-300mM before and after devazepide in wild-type mice. **(C-D)** Time to peak and area under the curve for CCK-870nM after devazepide and sucrose-300mM before and after devazepide ($n \geq 5$, error bars indicate S.E.M.). Statistics by ANOVA and Tukey HSD post hoc analysis.

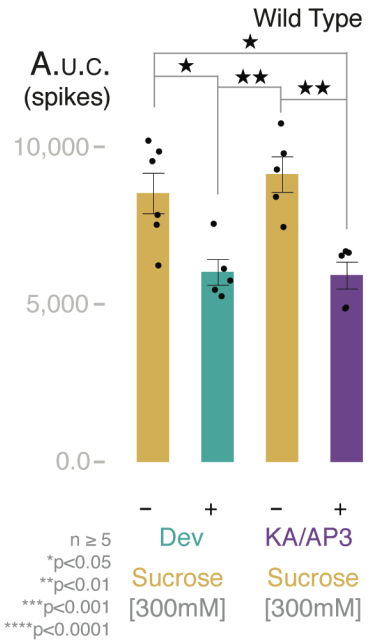

Fig. S19. Devazepide and glutamate inhibitor cocktail reduce the magnitude of vagal response to sucrose in wild-type mice. Area under the curve (A.U.C.) was calculated for each 6-minute vagal cuff recording to represent magnitude of response. Devazepide-2mg/kg and glutamate cocktail inhibitor (KA/AP3 = 150µg/kg kynurenic acid (KA) + 1mg/kg AP-3) were delivered and sucrose response was assessed after delivery. Both devazepide and glutamate inhibitor reduced A.U.C. ($n \geq 5$, error bars indicate S.E.M.). Statistics by ANOVA and Tukey HSD post hoc analysis.

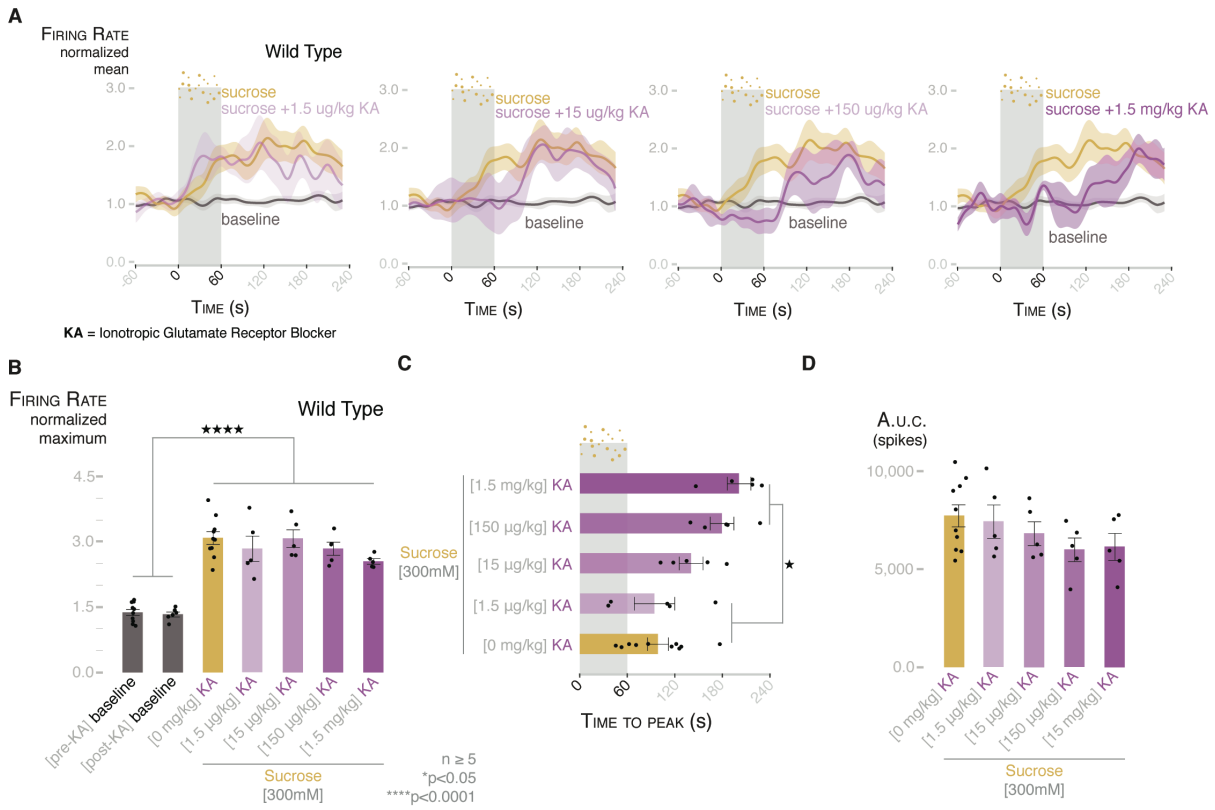

Fig. S20. Kynurenic acid (KA), an ionotropic glutamate receptor inhibitor, attenuates rapid vagal response but not prolonged vagal response to sucrose. **(A)** Normalized traces for baseline, sucrose-300mM, and sucrose-300mM after dose of KA: 1.5 µg/kg, 15 µg/kg, 150 µg/kg, and 1.5mg/kg. **(B)** Normalized maximum firing rate for baseline before and after KA, sucrose-300mM prior to KA, and sucrose-300mM after KA (doses above). **(C-D)** Time to peak and area under the curve (A.U.C.) for sucrose-300mM prior to KA and after KA (doses above). ($n \geq 5$, error bars indicate S.E.M.). Statistics by ANOVA and Tukey HSD post hoc analysis.

PROTEINS WITH HIGH EXPRESSION IN CCK SORTED CELLS

Primary protein name	Protein description	Number of quantified peptides	%CV QC pools	Fold-change	p-value t-test
GLUC_MOUSE	Glucagon GN=Gcg PE=1 SV=1	13	6.81	207.95	2.09E-06
GIP_MOUSE	Gastric inhibitory polypeptide GN=Gip PE=2 SV=2	20	2.29	194.03	4.20E-04
GHRL_MOUSE	Appetite-regulating hormone GN=Ghrl PE=1 SV=1	6	0.53	163.38	8.42E-04
CCKN_MOUSE	Cholecystokinin GN=Cck PE=1 SV=3	6	3.05	145.41	3.00E-03
TKN1_MOUSE	Protachykinin GN=Tac1 PE=2 SV=1	2	13.13	142.26	1.64E-05
SECR_MOUSE	Secretin GN=Sct PE=2 SV=1	8	1.71	71.19	7.50E-05
SMS_MOUSE	Somatostatin GN=Sst PE=2 SV=1	3	5.85	51.53	4.37E-04
NEUT_MOUSE	Neurotensin/neuromedin GN=Nts PE=2 SV=1	8	9.75	30.82	1.06E-04
CART_MOUSE	Cocaine-and amphetamine-regulated transcript protein GN=Cartpt PE=2 SV=2	2	7.10	20.67	2.00E-03
PYY_MOUSE	Peptide YY GN=Pyy PE=2 SV=2	4	2.36	17.96	3.14E-05
TPH1_MOUSE	Tryptophan 5-hydroxylase 1 GN=Tph1 PE=2 SV=1	1	20.66	14.48	3.6E-02

Table S1. Gut neuropeptides with high expression in intestinal Cck-GFP sorted cells compared to non-GFP intestinal epithelial cells. n=3 mice.

Movie S1. Two-photon z-stack from EnvA *ΔG*-rabies-GFP labeled nodose ganglion in which virus was delivered by enema into the colon of PyyCRE_rabG-TvA mouse.

Movie S2. Z-stack video of a PGP9.5-GFP neuron connecting to a CckCRE_tdTomato cell in an organoid co-culture.

Data S1. (separate file)
Spike Sorting Code used for vagal cuff recordings.

References and Notes

1. B. Alberts, D. Bray, J. Lewis, M. Raff, K. Roberts, J. D. Watson, *Molecular Biology of the Cell* (Garland, ed. 3, 1994), pp. 907–982.

2. A. Psichas, F. Reimann, F. M. Gribble, Gut chemosensing mechanisms. *J. Clin. Invest.* **125**, 908–917 (2015). doi:10.1172/JCI76309 Medline

3. J. B. Furness, L. R. Rivera, H. J. Cho, D. M. Bravo, B. Callaghan, The gut as a sensory organ. *Nat. Rev. Gastroenterol. Hepatol.* **10**, 729–740 (2013). doi:10.1038/nrgastro.2013.180 Medline

4. F. Feyrter, *Über diffuse endokrine epitheliale Organe* (J. A. Barth, Leipzig, Germany, 1938).

5. J. F. Rehfeld, The new biology of gastrointestinal hormones. *Physiol. Rev.* **78**, 1087–1108 (1998). doi:10.1152/physrev.1998.78.4.1087 Medline

6. D. Castaneda, F. Wang, A. J. Treichel, M. Streyle, K. R. Knutson, C. Bernard, H. J. Li, A. B. Leiter, G. Farrugia, A. Beyder, Mechanosensitive ION channel Piezo2 distribution in mouse small bowel and colon enterochromaffin cells. *Gastroenterology* **152**, S180 (2017). doi:10.1016/S0016-5085(17)30916-2

7. T. Braun, P. Voland, L. Kunz, C. Prinz, M. Gratzl, Enterochromaffin cells of the human gut: Sensors for spices and odorants. *Gastroenterology* **132**, 1890–1901 (2007). doi:10.1053/j.gastro.2007.02.036 Medline

8. H. J. Jang, Z. Kokrashvili, M. J. Theodorakis, O. D. Carlson, B.-J. Kim, J. Zhou, H. H. Kim, X. Xu, S. L. Chan, M. Juhaszova, M. Bernier, B. Mosinger, R. F. Margolskee, J. M. Egan, Gut-expressed gustducin and taste receptors regulate secretion of glucagon-like peptide-1. *Proc. Natl. Acad. Sci. U.S.A.* **104**, 15069–15074 (2007). doi:10.1073/pnas.0706890104 Medline

9. G. J. Rogers, G. Tolhurst, A. Ramzan, A. M. Habib, H. E. Parker, F. M. Gribble, F. Reimann, Electrical activity-triggered glucagon-like peptide-1 secretion from primary murine L-cells. *J. Physiol.* **589**, 1081–1093 (2011). doi:10.1113/jphysiol.2010.198069 Medline

10. D. V. Bohórquez, R. A. Shahid, A. Erdmann, A. M. Kreger, Y. Wang, *N.* Calakos, F. Wang, R. A. Liddle, Neuroepithelial circuit formed by innervation of sensory enteroendocrine cells. *J. Clin. Invest.* **125**, 782–786 (2015). doi:10.1172/JCI78361 Medline

11. *N.* W. Bellono, J. R. Bayrer, D. B. Leitch, J. Castro, C. Zhang, T. A. O'Donnell, S. M. Brierley, H. A. Ingraham, D. Julius, Enterochromaffin cells are gut chemosensors that couple to sensory neural pathways. *Cell* **170**, 185–198.e16 (2017). doi:10.1016/j.cell.2017.05.034 Medline

12. A. L. Haber, M. Biton, *N.* Rogel, R. H. Herbst, K. Shekhar, C. Smillie, G. Burgin, T. M. Delorey, M. R. Howitt, Y. Katz, I. Tirosh, S. Beyaz, D. Dionne, M. Zhang, R. Raychowdhury, W. S. Garrett, O. Rozenblatt-Rosen, H. *N.* Shi, O. Yilmaz, R. J. Xavier, A. Regev, A single-cell survey of the small intestinal epithelium. *Nature* **551**, 333–339 (2017). doi:10.1038/nature24489 Medline

13. L. L. Glass, F. J. Calero-Nieto, W. Jawaid, P. Larraufie, R. G. Kay, B. Göttgens, F. Reimann, F. M. Gribble, Single-cell RNA-sequencing reveals a distinct population of proglucagon-

expressing cells specific to the mouse upper small intestine. *Mol. Metab.* **6**, 1296–1303 (2017). doi:10.1016/j.molmet.2017.07.014 Medline

14. *N*. R. Wall, I. R. Wickersham, A. Cetin, M. De La Parra, E. M. Callaway, Monosynaptic circuit tracing in vivo through Cre-dependent targeting and complementation of modified rabies virus. *Proc. Natl. Acad. Sci. U.S.A.* **107**, 21848–21853 (2010). doi:10.1073/pnas.1011756107 Medline

15. S. M. Altschuler, J. Escardo, R. B. Lynn, R. R. Miselis, The central organization of the vagus nerve innervating the colon of the rat. *Gastroenterology* **104**, 502–509 (1993). doi:10.1016/0016-5085(93)90419-D Medline

16. E. K. Williams, R. B. Chang, D. E. Strochlic, B. D. Umans, B. B. Lowell, S. D. Liberles, Sensory neurons that detect stretch and nutrients in the digestive system. *Cell* **166**, 209–221 (2016). doi:10.1016/j.cell.2016.05.011 Medline

17. A. Sclafani, H. Koepsell, K. Ackroff, SGLT1 sugar transporter/sensor is required for post-oral glucose appetition. *Am. J. Physiol. Regul. Integr. Comp. Physiol.* **310**, R631–R639 (2016). doi:10.1152/ajpregu.00432.2015 Medline

18. F. Reimann, A. M. Habib, G. Tolhurst, H. E. Parker, G. J. Rogers, F. M. Gribble, Glucose sensing in L cells: A primary cell study. *Cell Metab.* **8**, 532–539 (2008). doi:10.1016/j.cmet.2008.11.002 Medline

19. G. Grabauskas, I. Song, S. Zhou, C. Owyang, Electrophysiological identification of glucose-sensing neurons in rat nodose ganglia. *J. Physiol.* **588**, 617–632 (2010). doi:10.1113/jphysiol.2009.182147 Medline

20. H. R. Berthoud, M. Kressel, H. E. Raybould, W. L. Neuhuber, Vagal sensors in the rat duodenal mucosa: Distribution and structure as revealed by in vivo DiI-tracing. *Anat. Embryol. (Berl.)* **191**, 203–212 (1995). doi:10.1007/BF00187819 Medline

21. L. R. Beutler, Y. Chen, J. S. Ahn, Y.-C. Lin, R. A. Essner, Z. A. Knight, Dynamics of gut-brain communication underlying hunger. *Neuron* **96**, 461–475.e5 (2017). doi:10.1016/j.neuron.2017.09.043 Medline

22. Z. Su, A. L. Alhadeff, J. *N*. Betley, Nutritive, post-ingestive signals are the primary regulators of AgRP neuron activity. *Cell Reports* **21**, 2724–2736 (2017). doi:10.1016/j.celrep.2017.11.036 Medline

23. C. Brandon, D. M. Lam, L-glutamic acid: A neurotransmitter candidate for cone photoreceptors in human and rat retinas. *Proc. Natl. Acad. Sci. U.S.A.* **80**, 5117–5121 (1983). doi:10.1073/pnas.80.16.5117 Medline

24. O. P. Ottersen, Y. Takumi, A. Matsubara, A. S. Landsend, J. H. Laake, S. Usami, Molecular organization of a type of peripheral glutamate synapse: The afferent synapses of hair cells in the inner ear. *Prog. Neurobiol.* **54**, 127–148 (1998). doi:10.1016/S0301-0082(97)00054-3 Medline

25. H. Haeberle, M. Fujiwara, J. Chuang, M. M. Medina, M. V. Panditrao, S. Bechstedt, J. Howard, E. A. Lumpkin, Molecular profiling reveals synaptic release machinery in Merkel cells. *Proc. Natl. Acad. Sci. U.S.A.* **101**, 14503–14508 (2004). doi:10.1073/pnas.0406308101 Medline

26. D. A. Berkowicz, P. Q. Trombley, G. M. Shepherd, Evidence for glutamate as the olfactory receptor cell neurotransmitter. *J. Neurophysiol.* **71**, 2557–2561 (1994). doi:10.1152/jn.1994.71.6.2557 Medline

27. J. S. Marvin, B. G. Borghuis, L. Tian, J. Cichon, M. T. Harnett, J. Akerboom, A. Gordus, S. L. Renninger, T.-W. Chen, C. I. Bargmann, M. B. Orger, E. R. Schreiter, J. B. Demb, W.-B. Gan, S. A. Hires, L. L. Looger, An optimized fluorescent probe for visualizing glutamate neurotransmission. *Nat. Methods* **10**, 162–170 (2013). doi:10.1038/nmeth.2333 Medline

28. I. R. Wickersham, D. C. Lyon, R. J. O. Barnard, T. Mori, S. Finke, K.-K. Conzelmann, J. A. T. Young, E. M. Callaway, Monosynaptic restriction of transsynaptic tracing from single, genetically targeted neurons. *Neuron* **53**, 639–647 (2007). doi:10.1016/j.neuron.2007.01.033 Medline

29. T. Sato, R. G. Vries, H. J. Snippert, M. van de Wetering, *N*. Barker, D. E. Stange, J. H. van Es, A. Abo, P. Kujala, P. J. Peters, H. Clevers, Single Lgr5 stem cells build crypt-villus structures in vitro without a mesenchymal niche. *Nature* **459**, 262–265 (2009). doi:10.1038/nature07935 Medline

30. Y. Wang, R. Chandra, L. A. Samsa, B. Gooch, B. E. Fee, J. M. Cook, S. R. Vigna, A. O. Grant, R. A. Liddle, Amino acids stimulate cholecystokinin release through the Ca^{2+}-sensing receptor. *Am. J. Physiol. Gastrointest. Liver Physiol.* **300**, G528–G537 (2011). doi:10.1152/ajpgi.00387.2010 Medline

31. S. Schonhoff, L. Baggio, C. Ratineau, S. K. Ray, J. Lindner, M. A. Magnuson, D. J. Drucker, A. B. Leiter, Energy homeostasis and gastrointestinal endocrine differentiation do not require the anorectic hormone peptide YY. *Mol. Cell. Biol.* **25**, 4189–4199 (2005). doi:10.1128/MCB.25.10.4189-4199.2005 Medline

32. Y. Shang, H. Wang, V. Mercaldo, X. Li, T. Chen, M. Zhuo, Fragile X mental retardation protein is required for chemically-induced long-term potentiation of the hippocampus in adult mice. *J. Neurochem.* **111**, 635–646 (2009). doi:10.1111/j.1471-4159.2009.06314.x Medline

33. P. Bäckström, P. Hyytiä, Ionotropic glutamate receptor antagonists modulate cue-induced reinstatement of ethanol-seeking behavior. *Alcohol. Clin. Exp. Res.* **28**, 558–565 (2004). doi:10.1097/01.ALC.0000122101.13164.21 Medline

34. M. Nawrot, A. Aertsen, S. Rotter, Single-trial estimation of neuronal firing rates: From single-neuron spike trains to population activity. *J. Neurosci. Methods* **94**, 81–92 (1999). doi:10.1016/S0165-0270(99)00127-2 Medline

35. *N*. Rakhilin, B. Barth, J. Choi, *N*. L. Muñoz, S. Kulkarni, J. S. Jones, D. M. Small, Y.-T. Cheng, Y. Cao, C. LaVinka, E. Kan, X. Dong, M. Spencer, P. Pasricha, *N*. Nishimura, X. Shen, Simultaneous optical and electrical in vivo analysis of the enteric nervous system. *Nat. Commun.* **7**, 11800 (2016). doi:10.1038/ncomms11800 Medline

36. M. M. Kaelberer, S. E. Jordt, A method to target and isolate airway-innervating sensory neurons in mice. *J. Vis. Exp.* **2016**, e53917 (2016). doi:10.3791/53917 Medline

37. A. J. Hughes, D. P. Spelke, Z. Xu, C.-C. Kang, D. V. Schaffer, A. E. Herr, Single-cell western blotting. *Nat. Methods* **11**, 749–755 (2014). doi:10.1038/nmeth.2992 Medline